

FAST TRACK COMMUNICATION

The origin of persistent spin dynamics and residual entropy in the stuffed spin ice $\text{Ho}_{2.3}\text{Ti}_{1.7}\text{O}_{7-\delta}$

H D Zhou¹, C R Wiebe^{1,2}, Y J Jo¹, L Balicas¹, Y Qiu^{3,4}, J R D Copley³,
G Ehlers⁵, P Fouquet⁶ and J S Gardner^{3,7}

¹ National High Magnetic Field Laboratory, Florida State University, Tallahassee, FL 32306-4005, USA

² Department of Physics, Florida State University, Tallahassee, FL 32306-3016, USA

³ NIST Center for Neutron Research, Gaithersburg, MD 20899-5682, USA

⁴ Department of Materials Science and Engineering, University of Maryland, College Park, MD 20742, USA

⁵ SNS Project, Oak Ridge National Laboratory, Oak Ridge, TN 37831-6475, USA

⁶ Institut Laue-Langevin, Boîte Postale 156X, F-38042, Grenoble Cedex 9, France

⁷ Indiana University, 2401 Milo B Sampson Lane, Bloomington, IN 47408, USA

E-mail: cwiebe@magnet.fsu.edu and jsg@nist.gov

Received 31 May 2007, in final form 5 July 2007

Published 20 July 2007

Online at stacks.iop.org/JPhysCM/19/342201

Abstract

The so-called ‘spin ices’ form when exchange interactions, crystal fields, and dipolar interactions are in a delicate balance. This gives rise to a ground state which has a considerable amount of residual spin entropy, much like the proton entropy in water ice through the freezing transition. Recently, ‘stuffed’ spin ices have provided a means to probe how delicate a balance is needed to stabilize the disordered ground state. Surprisingly, it is found that an increase of the density of spins results in very little change in the residual entropy, which leads to the interesting idea that residual entropy states might be more common than once believed for magnetism. In this communication, we detail the crystal growth of stuffed spin ice $\text{Ho}_{2.3}\text{Ti}_{1.7}\text{O}_{7-\delta}$, and we complete neutron scattering experiments to observe how the spins order at low temperatures. It is found that even with this large perturbation, the system still has some key signatures of the spin ice state, but the spin dynamics is significantly altered. With this new data, an explanation emerges for the zero-point entropy in the stuffed spin ices.

(Some figures in this article are in colour only in the electronic version)

In the spin ice $\text{Ho}_2\text{Ti}_2\text{O}_7$, Ho^{3+} , spins lie at the vertices of corner-shared tetrahedra within the pyrochlore lattice of $\text{Ho}_2\text{Ti}_2\text{O}_7$ [1–3]. Strong crystal field interactions restrict the spins to lying along the local $\langle 111 \rangle$ axes at low temperatures [4]. The magnetic exchange interactions are extremely weak—on the order of a few kelvins, which is approximately the same order

of magnitude for the dipolar interactions between Ho^{3+} spins. The resulting state at low temperatures is that each tetrahedron orders into a two-spin-in, two-spin-out configuration. However there is no long ranged order—the spins between adjacent tetrahedra are only loosely correlated through the spin vertex that they share. Long ranged dipolar forces stabilize the so-called ‘spin ice’ (SI) state which has a considerable amount of residual entropy [5]. Remarkably, the number of available states can be enumerated, and the resulting entropy is the same as the residual entropy due to proton disorder in water ice, providing a fascinating intersection between magnetism and solid-state chemistry [6]. ‘Stuffed spin ice’ (SSI), where extra magnetic ions replace the non-magnetic Ti^{4+} ions, was shown to have the same entropy per spin as the ‘unstuffed spin ice’ at low temperatures. This has provided the impetus to understand these exotic spin states [7, 8], and to synthesize large, high quality single crystals for detailed neutron scattering experiments.

Crystals of the stuffed spin ice $\text{Ho}_{2+x}\text{Ti}_{2-x}\text{O}_{7-\delta}$ were grown with the traveling floating-zone technique. Previously, powder samples were synthesized via a rapid cooling method, since the pyrochlore lattice is not stable to the additional insertion of large Ho^{3+} ions upon the Ti^{4+} sites [7]. The essential features of our method include: (1) very well defined melting zones, (2) high speed pre-scans of the polycrystalline rod before crystal growth, (3) an inert Ar atmosphere, and (4) narrow ceramic rods for the sample growth. Small pieces of the single crystals were ground into fine powder for x-ray diffraction (XRD). The room temperature measurements were recorded with an x-ray diffractometer equipped with Cu $K\alpha$ radiation. All the samples are single phase with a cubic structure. X-ray Laue diffraction was used to orient the crystal in the (H, H, L) plane. Neutron scattering measurements were completed at the NIST using the disk chopper spectrometer (DCS) and the neutron spin echo (NSE) spectrometer. Neutron spin echo experiments were also performed with the IN11 spectrometer at the Institut Laue-Langevin.

Figure 1(a) shows the XRD patterns for powder samples of $\text{Ho}_{2+x}\text{Ti}_{2-x}\text{O}_{7-\delta}$ with $x = 0.1$ and 0.3 that were synthesized with the image furnace. It is clear that with increasing Ho content, the pattern shifts to lower scattering angle which indicates that the lattice is increasing in size to accommodate the Ho^{3+} ions. The lattice parameter for $\text{Ho}_{2.3}\text{Ti}_{1.7}\text{O}_{7-\delta}$ is $a = 10.1745(2)$ Å, in agreement with the previously reported structure [7]. Crystals grown with this starting material resulted in well defined Laue patterns. The spots on the x-ray Laue pattern for a sample aligned along the $[111]$ axis confirm the high quality of the $\text{Ho}_{2.3}\text{Ti}_{1.7}\text{O}_{7-\delta}$ single crystal. The linear fit of the inverse susceptibility below 20 K yields a Curie–Weiss constant $\theta = 0.05$ K and an effective moment $\mu_{\text{eff}} = 10.5 \mu_B$, in agreement with previous results.

A 2 g crystal of $\text{Ho}_{2.3}\text{Ti}_{1.7}\text{O}_{7-\delta}$ was used for neutron scattering experiments down to 1.5 K. The three principal axes $[H, H, 0]$, $[0, 0, L]$ and $[H, H, H]$ were put in the scattering plane to provide a direct comparison with previously published $\text{Ho}_2\text{Ti}_2\text{O}_7$ data [9]. As the temperature was cooled, significant magnetic diffuse scattering was observed from the short ranged ordered Ho^{3+} spins.

The results are shown in figure 2. There are several important features to note about this data: (i) characteristic diffuse scattering typical of spin ices is observed, even with the random Ho^{3+} spins placed upon the interstitial sites [9]. This is surprising in light of the significant perturbation upon this system. Note that this data is quasielastic with an energy resolution of $-0.1 \text{ meV} < \Delta E < 0.1 \text{ meV}$, and is thus dominated by very slow spin fluctuations (slower than 20 GHz). (ii) The scattering near $Q = 0$ is a minimum. This indicates that antiferromagnetic (AF) interactions are still significant, consistent with susceptibility data [7]. (iii) Upon investigating the scattering in key symmetry directions, and comparing to $\text{Ho}_2\text{Ti}_2\text{O}_7$, some differences are noted. In the $[001]$ direction, for example, there are two broad peaks that are shifted from the commensurate positions of $(0, 0, 1)$ and $(0, 0, 3)$ to $(0, 0, 1.3)$ and

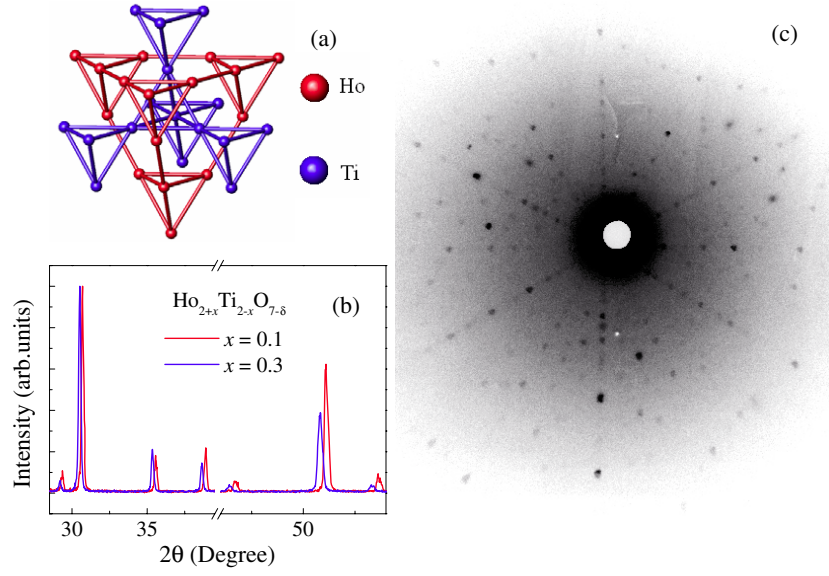


Figure 1. (a) The structure of $\text{Ho}_2\text{Ti}_2\text{O}_7$ ($\text{A}_2\text{B}_2\text{O}_7$) shown as a network of interpenetrating corner-shared tetrahedra. In the ‘stuffed spin ice’ state, extra Ho spins lie upon B-site positions. (b) Room temperature XRD patterns for $\text{Ho}_{2+x}\text{Ti}_{2-x}\text{O}_{7-\delta}$ with $x = 0.1$ (red) and $x = 0.3$ (blue). (c) X-ray Laue pattern along $[111]$ axis for single-crystal $\text{Ho}_{2.3}\text{Ti}_{1.7}\text{O}_{7-\delta}$.

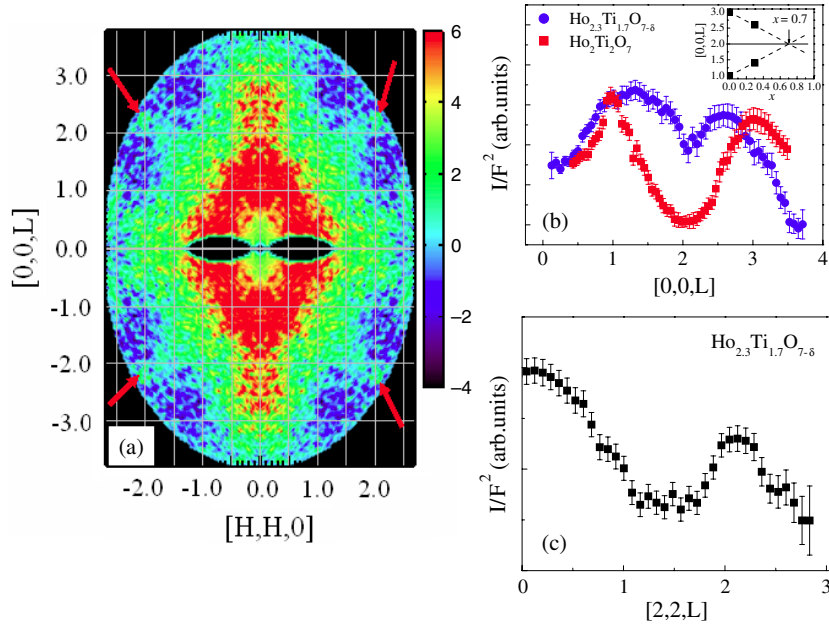


Figure 2. (a) Experimental elastic ($\Delta E = -0.1$ to 0.1 meV) neutron scattering pattern of $\text{Ho}_{2.3}\text{Ti}_{1.7}\text{O}_{7-\delta}$ in the (H, H, L) plane at $T = 1.5$ K. The data has been folded along the $(H, H, 0)$ and $(0, 0, L)$ axes. (b) Cuts along the $[00L]$ direction for the stuffed spin ice (SSI) and the unstuffed spin ice. The inset shows the shift in the diffuse scattering peaks towards the $[002]$ direction. (c) Cut along $[22L]$ for the SSI, emphasizing the ‘pinch points’ at $[222]$ marked by arrows in (a).

(0, 0, 2.7) (figure 2). This is a key signature of competing interactions that are introduced with Ho^{3+} doping. Monte Carlo simulations from previous work can reproduce these results with the dipolar spin ice model, which assumes that the dipolar forces play a role along with magnetic exchange [9]. A physical interpretation of these diffuse scattering peaks in $\text{Ho}_2\text{Ti}_2\text{O}_7$ is that they correspond to symmetry-forbidden locations within the face centered cubic pyrochlore structure—all of the indices must be odd or even for face centered cubic (FCC) lattices. These peaks are all indicative of AF correlations which break the FCC symmetry. In contrast, the $\text{Ho}_{2.3}\text{Ti}_{1.7}\text{O}_{7-\delta}$ sample has peaks that are removed from these positions, and shifted towards the (002) position by the same amount. The interactions between the spins are shifting from AF to FM as the system is doped. (iv) In the $\langle 222 \rangle$ directions, characteristic ‘pinch point’ scattering centers are observed where the scattering becomes well defined at certain \mathbf{Q} wavevectors [3]. These features were previously interpreted as a direct consequence of the long ranged dipolar forces within the spin ice system [10]. In the stuffed spin ice, therefore, strong dipolar interactions survive with Ho^{3+} doping.

Based upon these observations, what can be concluded about the nature of the ground state in the stuffed spin ice? From the diffuse scattering, it is clear that the majority of the spins are still frozen within a slightly altered, but still ice-like configuration. The correlations are more ferromagnetic, and the pattern is not as distinct as the unstuffed spin ice, but it is clear that long ranged dipolar forces are still defining the nature of the spins at low temperatures. To determine over which timescales the spins are fluctuating, we have completed inelastic neutron scattering experiments and spin echo experiments on a larger, 15 g, polycrystalline sample. Figures 3(a)–(c) show a false contour color plot of the scattering function $S(\mathbf{Q}, \omega)$ at various temperatures. In figure 3(d), the results of the integrated intensity scans are shown as a function of temperature, comparing the spin ice state to the stuffed spin ice at low temperatures. Note that the spin ice is largely static within the neutron timescale. This is clear from the spin echo experiments as well, which show little relaxation at low temperatures compared to paramagnetic spins with some relaxation at 100 K [11]. This is in direct contrast to the stuffed spin ice, which has a build-up of low energy excitations as the temperature is cooled. These have a characteristic energy scale of $\sim 0.5 \text{ meV} \sim 5 \text{ K}$ (figures 3(a)–(c)). The dynamic nature of these spins is also evident within the spin echo measurements, which show little change in the relaxation as the sample is cooled, indicating a much more dynamic spin system at low temperatures. The SSI data in figure 3(e) has been fit to a stretched exponential function, which has also been used to describe the slowly fluctuating spins in related frustrated systems such as the kagomé bilayer compound $\text{Ba}_2\text{Sn}_2\text{ZnCr}_{7x}\text{Ga}_{10-7x}\text{O}_{22}$ (BSZCGO) [12].

Therefore, although the diffuse scattering observed in a diffraction experiment suggests that a significant number of spins are frozen within the ‘ice-like’ configurations on each tetrahedra, the inelastic neutron scattering measurements conclusively show that the spin system is very dynamic, or fluctuating, down to $T = 50 \text{ mK}$. Since these spin excitations are absent in the spin ice state, but present in the stuffed spin ice state and they coexist with the diffuse scattering features within the stuffed spin ice, these excitations are likely due to the unpaired spins upon the B-sites. They are only loosely correlated with each other, with little or no- $|\mathbf{Q}|$ dependence, but typical of spin excitations in other frustrated systems such as the kagomé $\text{SrCr}_{9x}\text{Ga}_{12-9x}\text{O}_{19}$ (SCGO) [13]. In fact, these dispersionless modes in SCGO are attributed to small clusters of spins which are decoupled from the rest of the system [13]. The extra intensity at low $|\mathbf{Q}|$ of these modes (figures 3(a)–(c)) indicates that these excitations are FM in nature, which is consistent with the picture of added FM correlations building up with extra stuffed spins on the B-sites.

What can now be said about the residual entropy in the stuffed spin ices? Lau *et al* find that the entropy per Ho^{3+} spin in the stuffed spin ices remains essentially constant across the

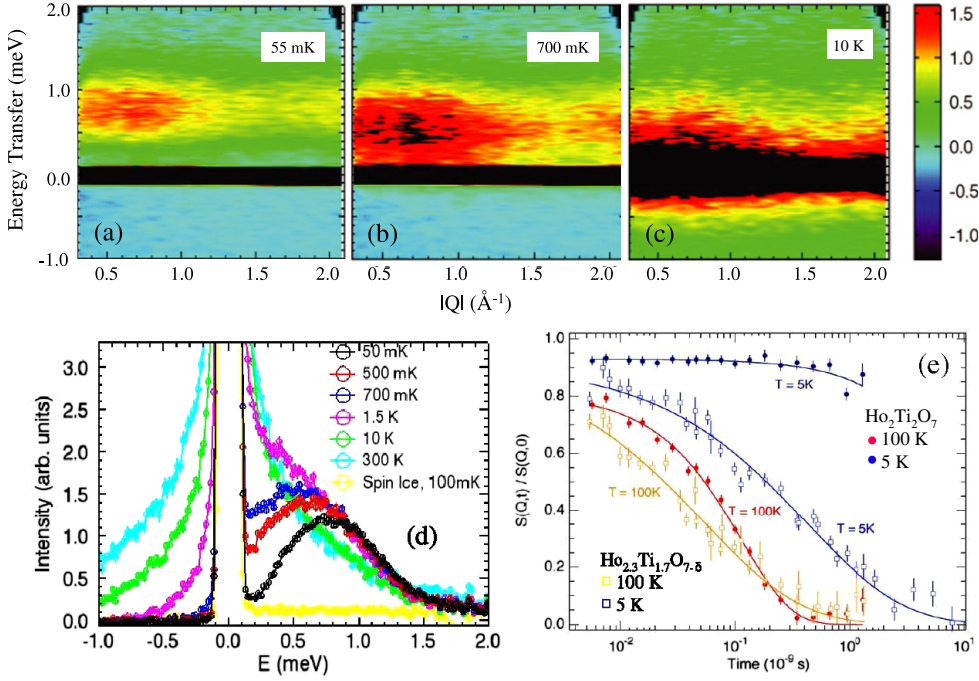


Figure 3. (a) Inelastic neutron scattering experiments on the $x = 0.3$ stuffed spin ice at (a) 55 mK (b) 700 mK and (c) 10 K, noting the appearance of a gapped spin excitation at low temperatures. (d) Cuts as a function of energy through this mode at various temperatures. Note the comparison to the static unstuffed spin ice. (e) Neutron spin echo results on stuffed and unstuffed spin ice. Within the neutron time window, the spin ice appears static by 5 K (90% of the spin are static), but the stuffed spin ice has persistent dynamics. The spin ice data have been fit to an exponential relaxation function, and the SSI data have been fit to a stretched exponential as guides to the eye.

entire series of dopants, suggesting that the ‘stuffed’ spins somehow obey the ice rules even though they lie in different crystal environments [7]. To test this, we made our own specific heat measurements on our crystals. The measured specific heat for $\text{Ho}_{2.3}\text{Ti}_{1.7}\text{O}_{7-\delta}$ is plotted in figure 4. The magnetic specific heat is obtained by subtracting the lattice contribution and the low temperature Schottky peak associated with the nuclear hyperfine contributions, using the fits obtained by previous works [7]. The magnetic entropy $S(T)$ at $H = 0$ and 1 T was calculated by integrating $C_{\text{magnetic}}(T)/T$. The calculations assume that $S = 0$ at $T = 0$ K. At $H = 0$ T, the integrated entropy at high temperature is only slightly higher ($S = 4.3 \text{ J K}^{-1} \text{ mol}^{-1}$) than $S = R[\ln 2 - 1/2 \ln(3/2)] = 4.1 \text{ J K}^{-1} \text{ mol}^{-1}$, the value previously obtained using the ice rules [7]. The residual entropy is rather robust with respect to an applied magnetic field of $H = 1$ T, also in agreement with previous measurements [7]. What is the origin of this residual entropy in the stuffed spin ices? Based on our neutron results, we suggest a different interpretation than Lau *et al.* The spins upon the A-sites in the SSI certainly have all the characteristics of the spin ices—they have similar diffuse scattering profiles, heat capacity behavior, and DC susceptibility, albeit with a shift towards more FM correlations as evidenced through our neutron scattering experiments. These extra correlations are brought about through the dipolar fields of the extra Ho^{3+} spins randomly distributed upon the B-sites. The entropy contribution from the B-site spins is expected to be different than the A-sites. They lie at different locations within the unit cell, and therefore should have different

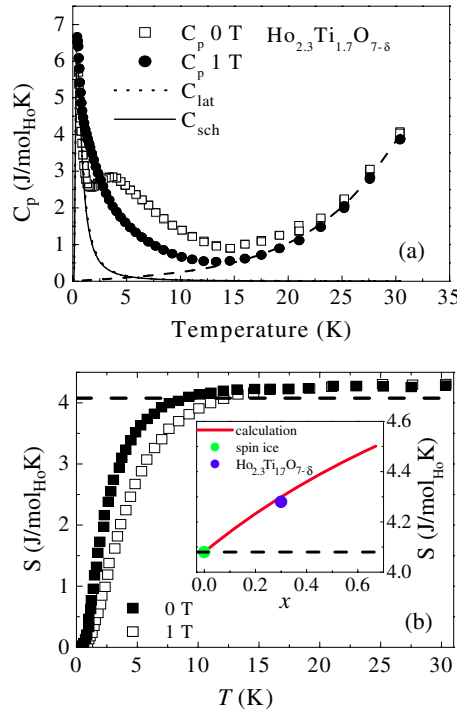


Figure 4. (a) Heat capacity of the stuffed spin ice as a function of temperature and applied fields. The lattice fit and low T Schottky anomalies have been calculated according to Lau [6]. (b) The extracted entropy/spin of the stuffed spin ice, which is slightly higher than the unstuffed spin ice result (dashed line). The inset shows that entropy/spin of the stuffed spin ice compared to the unstuffed spin ice. The solid line is the calculation in the text with the B-site 'orphan spin' model.

crystal field schemes. However, the spins on the B-site should still have an Ising-like character with a ground state doublet. In this scenario, the Ho^{3+} spins upon the B-site behave as loosely correlated paramagnetic spins with a characteristic energy scale. With the assumption that these spins can be modeled with a simple two-level system with an energy scale of 5 K separating the two spin states, the total amount of entropy associated with these spins would then be $R \ln 2 = 5.54 \text{ J K}^{-1} \text{ mol}^{-1}$. Therefore, the total amount of integrated entropy per spin, for the $x = 0.3$ case, would be

$$S = \frac{S(\text{spin ice}) + S(\text{unpaired spins})}{2.3} \quad (1)$$

$$S = \frac{2(R(\ln 2 - \frac{1}{2}\ln(3/2))) + 0.3(R \ln 2)}{2.3} = 4.3 \text{ J K}^{-1} \text{ mol}^{-1}. \quad (2)$$

This agrees with the value obtained from Lau *et al* ($S = 4.3 \text{ J K}^{-1} \text{ mol}^{-1}$), and also within agreement with our results (figure 4) [7]. We therefore suggest that the excess residual entropy in the stuffed spin ice state is due to the unpaired Ho^{3+} spins which are not in a spin ice configuration. In figure 4, we make this point by plotting the entropy as a function of doping across the series. Note that there is only a slight increase in the entropy using the 'orphan spin' argument, which agrees with the general trend from previous results [7].

From our measurements on the first reported crystals of the 'stuffed spin ice', it appears that the unusual result of the excess residual entropy/spin can be explained through the remaining

fluctuating Ho^{3+} spins upon the B-sites that do not follow the ice rules. These spins shift the correlations of the ice state on the A-site to a ferromagnetic character, and it has been demonstrated that this new ground state is more dynamic than the traditional ‘frozen’ ice state. The details of the complete spin excitation spectrum should reveal how the ‘orphan’ B-site spins interact with the lattice and reveal more differences between the two ice systems. It is curious that ‘stuffing’ the system with extra spins seems to ‘free’ up the dynamics. It has been predicted that the opposite approach, that of adding diamagnetic impurities to the system, would have this effect much like doping water ice with KOH leads to new ordered phases [1, 14]. ‘Stuffing’ lattices with extra spins might yield a similar result, leading to new magnetic phases at higher doping levels.

There remains the possibility that the new modes that we are observing in the ‘stuffed spin ice’ are not from the B-site model we have suggested, and are in fact due to collective modes of a more dynamic ice system as a whole. The diffuse scattering would then have to be interpreted as short ranged correlations of a dynamic system which could explore all possible spin configurations over long enough timescales. Such a system, expected to be ergodic, should have no residual entropy as it will eventually find an ordered ground state that will be a global minimum of its free energy [15]. It would appear, then, that this system would have a dynamic, fluctuating ground state, much like other rare-earth pyrochlores such as the spin liquid $\text{Tb}_2\text{Ti}_2\text{O}_7$ [16]. More detailed neutron scattering experiments are needed on a wide variety of dopings to verify this scenario. The realization of the spin liquid within the ‘stuffed spin ice’ (in effect, melting the ice state through the increased density of spins) is a fascinating avenue towards a dynamic state which would seem to violate the third law of thermodynamics.

This work was made possible by support through the NSF (DMR-0084173 and DMR-0454672), the EIEG program (FSU) and the auspices of the state of Florida. ORNL/SNS is managed by UT-Battelle, LLC, for the Department of Energy under contract DE-AC05-00OR227225. We thank the technical support from the staff at NIST and the ILL. Data analysis was completed with DAVE, which can be obtained at <http://www.ncnr.nist.gov/dave/>.

References

- [1] Bramwell S T *et al* 2001 *Science* **294** 1495
- [2] Greedan J E 2000 *J. Mater. Chem.* **11** 37
- [3] Moessner R *et al* 2006 *Phys. Today* **59** 24
- [4] Harris M J *et al* 1997 *Phys. Rev. Lett.* **79** 2554
- [5] den Hertog B C *et al* 2000 *Phys. Rev. Lett.* **84** 3430
- [6] Pauling L 1935 *J. Am. Chem. Soc.* **57** 2680
- [7] Lau G C *et al* 2006 *Nat. Phys.* **2** 249
- [8] Lau G C *et al* 2006 *J. Solid State Chem.* **179** 3126
- [9] Bramwell S T *et al* 2001 *Phys. Rev. Lett.* **87** 047205
- [10] Zinkin M P *et al* 1997 *Phys. Rev. B* **56** 11786
- [11] Ehlers G *et al* 2003 *J. Phys.: Condens. Matter* **15** L9
- [12] Mutka H *et al* 2006 *Phys. Rev. Lett.* **97** 047203
- [13] Lee S-H *et al* 1996 *Phys. Rev. Lett.* **76** 4424
- [14] Tajima Y *et al* 1982 *Nature* **299** 810
- [15] Goldenfeld N 2005 *Lectures on Phase Transitions and the Renormalization Group* (New York: Westfield Press)
- [16] Gardner J S *et al* 1999 *Phys. Rev. Lett.* **82** 1012